# Adsorption Behavior and Mechanism of 2,4,6-Trichlorophenol on Nut Shell Activated Carbon

Liming Cao,[a,b,c] Yan Li,[a,b,c] Xiaorong Mo,[a,b,c] Jing Li,[a,b,c] Qin Wu,[a,c] and Shuangquan Yao [a,b,c,]*

The adsorbable organic halides (AOX) produced during chlorine dioxide bleaching are highly toxic and difficult to degrade. Currently, AOX generation is mainly reduced by controlling conditions during bleaching. Studies on AOX removal in the natural environment are rarely reported. In this study, the adsorption of 2,4,6-trichlorophenol (2,4,6-TCP) on nut shell activated carbon was investigated. The effects of activated carbon dosage, adsorption time, and temperature on the removal of 2,4,6-TCP were examined. The optimal adsorption conditions was activated carbon dosage 0.20 g × L$^{-1}$, adsorption time 130 min, and temperature 25 °C. The removal efficiency of 2,4,6-TCP was 91.5%. The adsorption kinetics and isothermal adsorption were studied, and a thermodynamic equation was established. The adsorption was more consistent with a pseudo-second-order kinetic model and Freundlich adsorption isotherm model. Thermodynamic studies showed that the adsorption of 2,4,6-TCP on activated carbon was a spontaneous exothermic process. These findings provide a new method for AOX removal in natural environments.

*Keywords: Activated carbon; 2,4,6-TCP; Removal efficiency; Adsorption kinetics; Thermodynamics*

*Contact information: a: State Key Laboratory of Biobased Material and Green Papermaking, Qilu University of Technology, Shandong Academy of Sciences, Jinan, 250353, PR China; b: School of Light Industrial and Food Engineering, Guangxi University, Nanning, 530004, PR China; c: Guangxi Key Laboratory of Clean Pulp & Papermaking and Pollution Control, Nanning, 530004, PR China;*
** Corresponding author: yaoshuangquan@sina.cn*

## INTRODUCTION

Adsorbable organic halides (AOX) are persistent organic pollutants in bleaching effluents and are highly toxic and difficult to degrade (Jaacks and Staimez 2015; Yao *et al.* 2015; Zhang *et al.* 2019). Their accumulation in natural environments (Krawczyk *et al.* 2013) can damage the environment and human health (Savant *et al.* 2006; Krawczyk *et al.* 2013). Therefore, several researchers have studied the formation mechanism of AOX in chlorine dioxide bleaching to reduce the formation of AOX from the source (Nie *et al.* 2014; Yao *et al.* 2015).

Currently, optimization, chemical treatment, and biological treatment are the main methods employed to reduce concentrations of AOX in effluent from pulp and paper mills (Nie *et al.* 2018; Ge *et al.* 2020; Huang *et al*. 2020). The contents of dioxin and organochloride are noticeably reduced by gas-phase lignin removal technology (Terrell *et al.* 2020). Adsorbable organic halides are mainly generated from lignin and hemicellulose (Yao *et al.* 2017; Shi *et al.* 2019). These components can be removed by different pretreatment methods. Therefore, AOX reduction by chemical treatment has been investigated. Francis *et al.* (1997) studied the effect of pretreatment by alkaline sulfides on woody biomass, and AOX content decreased by 30%. Deshmukh *et al.* (2009) studied the effects of acetate and glucose on the biodegradation of AOX. The degradation of AOX was noticeably improved by the addition of electron donors, such as acetic acid and glucose into the bleaching system.

At present, elemental chlorine free (ECF) bleaching with chlorine dioxide as the main bleaching agent is one of the main bleaching technologies. Formation of AOX has been significantly reduced using this technique. However, due to the limitations of the main chlorine dioxide preparation technology, a small amount of AOX is still generated during chlorine dioxide bleaching (Liu *et al*. 2020). AOX is generated from the reaction between chlorine gas and lignin, as well as with hexenuronic acid in the unbleached pulp (Yao *et al.* 2016; Shi *et al.* 2019). With the discharge of pulp and paper wastewater, AOX discharged into the natural environment is continuously accumulating, and the threat to the environment is also increasing. At present, the mechanism of AOX generation during bleaching has attracted much attention. There have been efforts to reduce AOX generation at source by optimization of the pulp bleaching process. However, there have been few reports on the removal of AOX that has been discharged into the natural environment. Activated carbon, which is an excellent adsorbent, has been widely used to adsorb organic pollutants (Vikrant *et al.* 2020) and heavy metals (Kadirvelu *et al.* 2001). Nut shell activated carbon has unique physical and chemical properties, such as high specific surface area, excellent hydrophobicity, and porous structure (Bhatnagar *et al.* 2013; Fernandez *et al.* 2014), and it is widely used as an adsorbent in water purification, gas separation, and industrial catalysis (Amstaetter *et al.* 2012; Ceyhan *et al.* 2013; Šmídová *et al.* 2017). Therefore, the adsorption of AOX on nut shell activated carbon is of great significance.

Chlorobenzene and chlorophenol are typical components of AOX. In this study, as a model compound of AOX, the adsorption of 2,4,6-TCP on nut shell activated carbon was studied. The effects of activated carbon dosage, adsorption time, and temperature on the removal efficiency of 2,4,6-TCP were investigated. The adsorption mechanism of 2,4,6-TCP on activated carbon was determined by examining various adsorption kinetic models, adsorption isotherms, and adsorption thermodynamic models. The results provide a new method for AOX removal in natural environment.

## EXPERIMENTAL

### Materials

Nut shell activated carbon (30 mesh to 60 mesh) was purchased from Aladdin Biotechnology Co., Ltd. (Shanghai, China). Analytical grade 2,4,6-TCP was obtained from Sigma-Aldrich (St. Louis, MO, USA). Other analytical reagents were purchased from Aladdin Biotechnology Co., Ltd. (Shanghai, China). All chemicals used were of analytical grade.

### Methods

An ultraviolet visible (UV-vis) spectrophotometer (SPECORD 50 PLUS; Analytik Jena AG, Analytikjena, Germany) was used to determine the absorption spectra. The absorption spectrum of 2,4,6-TCP had a characteristic peak at 204 nm, and no peaks corresponding to other interfering substances in the solution were observed. The equation of the standard curve for the absorbance at 204 nm was as follows (Eq. 1). This equation was used to analyze the concentration of 2,4,6-TCP in the reaction solution.

$$y = 0.2269\,x \qquad (R^2 = 0.9996) \tag{1}$$

Activated carbon samples of different weights were placed into conical flasks, each of which contained 100 mL of pure water. Various concentrations of 2,4,6-TCP solutions were added to the flasks. The mixture was shaken, and adsorption was allowed to proceed in a constant temperature oscillator at different temperatures and for different time periods. The 2,4,6-TCP concentrations in the reaction solutions were measured. Each sample was measured three times and averaged.

The adsorption capacity of activated carbon for 2,4,6-TCP was calculated using Eq. 2,

$$Q = (C_0 - C)V / m \times 100\% \tag{2}$$

where $C_0$ (mg × $L^{-1}$) is the initial concentration of 2,4,6-TCP. $C$ (mg × $L^{-1}$) is the concentration of 2,4,6-TCP after adsorption. $V$ (L) is the solution volume. $m$ (g) is the activated carbon dosage. $Q$ (mg × $g^{-1}$) is the adsorption capacity of activated carbon.

The specific surface area of activated carbon with and without adsorption of 2,4,6-TCP was measured using a BET specific surface area analyzer (ASAP 2460, MICROMERITICS, United States). The test environment had a relative pressure of 0.975 MPa and a temperature of 77 K.

The micromorphological changes of 2,4,6-TCP adsorbed by activated carbon were observed by field emission scanning electron microscope (FE-SEM, Hitachi SU8010, Japan). The moisture in activated carbon samples was removed before the test, and the activated carbon was sprayed with gold to improve its electrical conductivity.

## RESULTS AND DISCUSSIONS

### Effect of Activated Carbon Dosage on the Removal of 2,4,6-TCP

Activated carbon dosage has a noticeable effect on the adsorption behavior of activated carbon (Bhatnagar *et al.* 2013). Therefore, the effects of activated carbon dosage on its adsorption capacity and the removal of 2,4,6-TCP were studied. The activated carbon dosage was increased from 0.03 g × $L^{-1}$ to 0.50 g × $L^{-1}$. The initial 2,4,6-TCP concentration, temperature, and time duration were 7.00 mg × $L^{-1}$, 25 °C, and 130 min, respectively. The results are shown in Fig. 1. The error bar is the standard deviation.

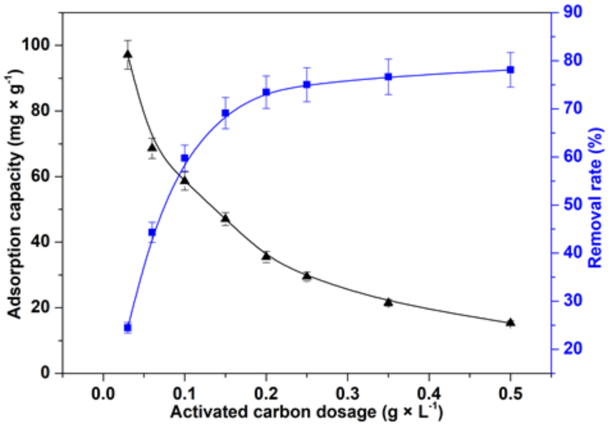

**Fig. 1.** Effect of activated carbon dosage on the adsorption capacity of activated carbon and the removal rate of 2,4,6-TCP

Figure 1 shows that the 2,4,6-TCP removal increased as activated carbon dosage increased at dosages less than 0.20 g × L$^{-1}$. The removal was 24.5% at an activated carbon dosage of 0.03 g × L$^{-1}$. It increased to 73.4% when the dosage was 0.20 g × L$^{-1}$. This is due to the loose porous activated carbon, there are many adsorption sites on the surface (Wirasnita *et al.* 2018). As activated carbon dosage increased, more active sites were available to adsorb 2,4,6-TCP. Therefore, the 2,4,6-TCP removal increased rapidly in the early stages of adsorption. However, increased activated carbon dosages also lead to the blockage of sites by activated carbon particles (Zhang *et al.* 2007). The surface area of the nut shell activated carbon is 1077 m$^2$ × g$^{-1}$. Its specific surface area after adsorption saturation is 148 m$^2$ × g$^{-1}$ at the dosage of 0.20 g × L$^{-1}$. The significant reduction in specific surface area means that it had little influence on 2,4,6-TCP removal at dosage exceeding 0.20 g × L$^{-1}$. Therefore, the 2,4,6-TCP removal remained unchanged when the activated carbon dosage was higher than 0.20 g × L$^{-1}$. The adsorption capacity of activated carbon decreased from 97.13 mg × g$^{-1}$ to 15.33 mg × g$^{-1}$. This was because the unsaturated adsorption sites on activated carbon increase as dosage increases (Hameed *et al.* 2008). The adsorption capacity of activated carbon decreased as dosage increased at a constant 2,4,6-TCP concentration. The optimal activated carbon dosage was 0.20 g × L$^{-1}$.

## Effect of Adsorption Time on the Removal of 2,4,6-TCP

The adsorption capacity of activated carbon increased as adsorption time increased and ultimately reached saturation. The effect of adsorption time on the removal of 2,4,6-TCP was studied. Adsorption was allowed to proceed for 5 min, 15 min, 30 min, 60 min, 100 min, 130 min, and 210 min. The activated carbon dosage, initial 2,4,6-TCP concentration, and reaction temperature were 0.20 g × L$^{-1}$, 7.00 mg × L$^{-1}$, and 25 °C, respectively. The results are shown in Fig. 2.

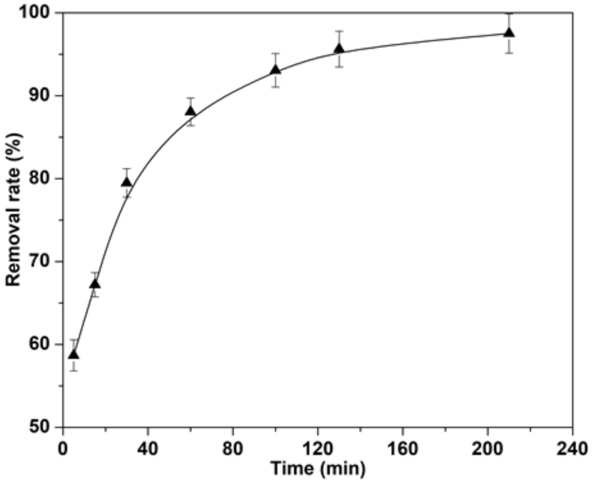

**Fig. 2.** Effect of adsorption time on the removal of 2,4,6-TCP

Figure 2 shows that the removal of 2,4,6-TCP increased rapidly for adsorption times at 60 min. The removal was 58.7% at 5 min and increased to 88.1% at 60 min. The removal continued to increase, but the growth gradually decreased between 60 min and 130 min. The removal was 95.6% at 130 min and remained stable thereafter. This was due to the fact that the adsorption of chlorophenols on activated carbon can be roughly divided into three stages (Shih *et al.* 2003; Tan *et al.* 2009). The 2,4,6-TCP was quickly adsorbed on activated carbon, as its surface has strong binding sites. The 2,4,6-TCP surface active sites were occupied as adsorption time increased, and the molecules diffused from the surface to the interior of the adsorbent. Therefore, the extent of removal increase gradually decreased between 60 min and 130 min. Active sites on the surface and interior of activated carbon were gradually occupied. This is consistent with SEM analysis. SEM of activated carbon raw materials and activated carbon with the adsorption saturation state is shown in Fig. 3. Compared with activated carbon raw material, the surface of activated carbon after adsorption was more dense. Much of its porosity disappeared due to filling by 2,4,6-TCP. As the pores and active adsorption points on the activated carbon surface became occupied, adsorption saturation was reached. Further increase of adsorption time had no significance for the removal of 2,4,6-TCP. The adsorption reached saturation after 130 min, which indicated that the optimal adsorption time was 130 min.

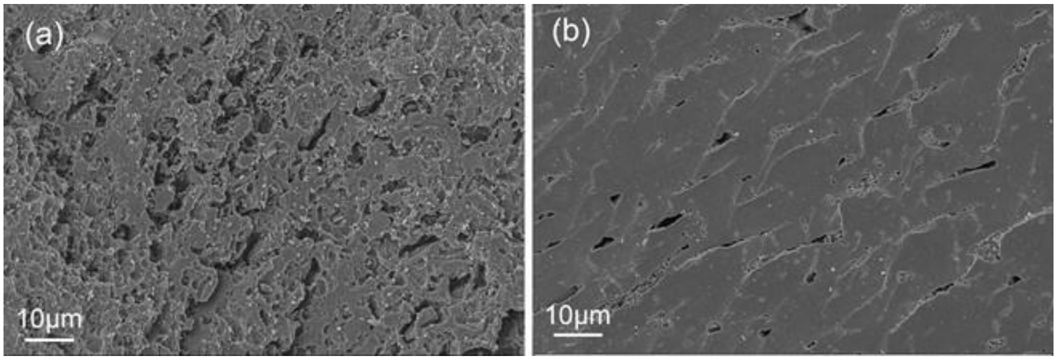

**Fig. 3.** SEM of activated carbon with and without adsorption 2,4,6-TCP (a, raw material of activated carbon, b, activated carbon adsorption 2,4,6-TCP in the adsorption saturated state)

## Effect of Temperature on the Removal of 2,4,6-TCP

The effect of temperature on the adsorption of 2,4,6-TCP on activated carbon was studied, and results are shown in Fig. 4. Adsorption temperatures of 15 °C, 25 °C, 35 °C, 50 °C, and 70 °C were examined. The activated carbon dosage, initial 2,4,6-TCP concentration, and reaction time were 0.20 g × $L^{-1}$, 7.00 mg × $L^{-1}$, and 130 min, respectively.

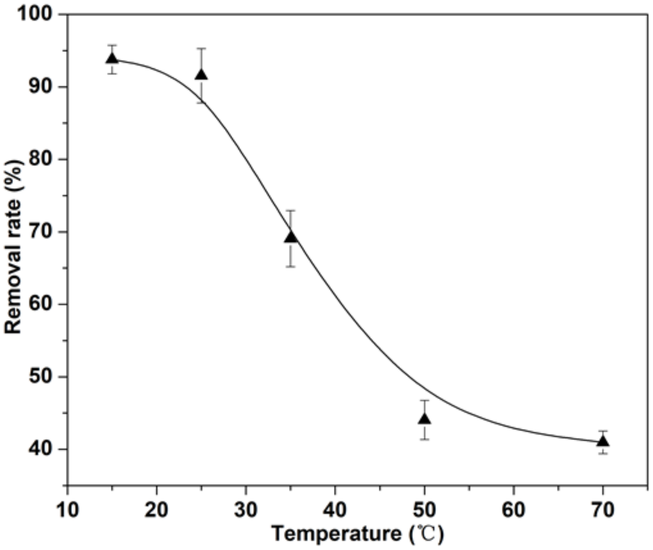

**Fig. 4.** Effect of temperature on the removal of 2,4,6-TCP

The removal of 2,4,6-TCP decreased as temperature increased. It decreased rapidly from 93.8% to 41.0% when temperature was increased from 15 °C to 70 °C. This was because adsorption on activated carbon is generally exothermic in nature (You *et al.* 2017). The removal of 2,4,6-TCP decreased at high temperatures, as high temperatures were not favorable for adsorption on activated carbon. The removal of 2,4,6-TCP at 15 °C and 25 °C were 93.8% and 91.5%, respectively. This suggested that the extent of removal increase is lower at temperatures below 25 °C. Thus, the optimal temperature was 25 °C.

## Adsorption Kinetics

Analysis of the adsorption kinetics can explain the reaction mechanism and reaction pathway and can predict the adsorption sequence based on adsorption kinetic models. The adsorption data were fit to three adsorption kinetic models, which included a pseudo-first-level model, a pseudo-second-level model, and the Elovich model (Kavitha and Namasivayam 2007; Zhang *et al.* 2012). The adsorption mechanism of 2,4,6-TCP on activated carbon was investigated, and the results are shown in Fig. 5. The pseudo-first-order model, the pseudo-second-order model, and the Elovich model were expressed using Eqs. 3, 4, and 5, respectively,

$$\mathrm{Lg}(Q_\mathrm{e} - Q_\mathrm{t}) = \mathrm{lg}Q_\mathrm{e} - k_1 t / 2.303 \tag{3}$$

$$t / Q_\mathrm{t} = 1 / (k_2 Q_\mathrm{e}^2) + t / Q_\mathrm{e} \tag{4}$$

$$Q_\mathrm{t} = 1 / \beta \ln(\alpha\beta) + 1 / \beta \ln t \tag{5}$$

where $Q_\mathrm{e}$ and $Q_\mathrm{t}$ (mg × $\mathrm{g}^{-1}$) are the amounts adsorbed at equilibrium and after time $t$, respectively, on the activated carbon. $k_1$ and $k_2$ are the pseudo-first-order and quasi-second-order constants of the kinetic models, respectively. $\alpha$ (mg × $\mathrm{g}^{-1}$ × $\mathrm{min}^{-1}$) is the initial adsorption rate. $\beta$ (g × $\mathrm{mg}^{-1}$) is an analytical constant.

**Table 1.** Kinetic Parameters for the Adsorption of 2,4,6-TCP on Activated Carbon

| Model | Fitted Equation | $R^2$ | $Q_\mathrm{e}$ (mg × $\mathrm{g}^{-1}$) | *K* | *α* | *β* |
|---|---|---|---|---|---|---|
| Pseudo-first | *y* = -0.0074*x* + 1.1010 | 0.9915 | 12.00 | 31.87 | / | / |
| Pseudo-second | *y* = 0.0311*x* + 0.2563 | 0.9987 | 31.87 | 0.0048 | / | / |
| Elovich | *y* = 3.377*x* + 13.50 | 0.9875 | / | / | 183.90 | 0.2961 |

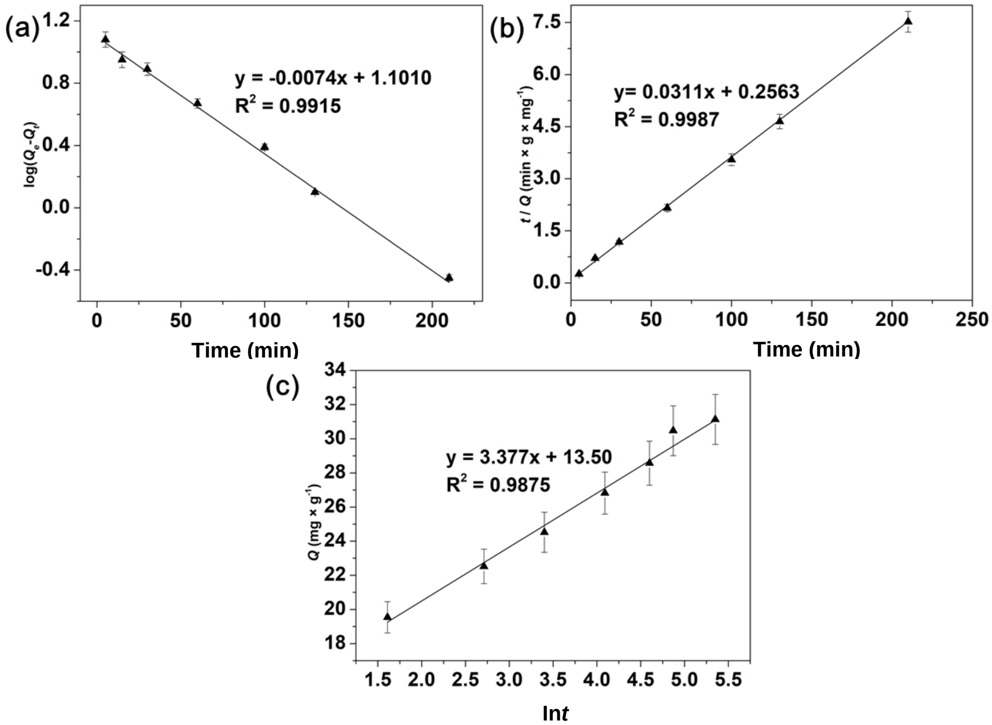

**Fig. 5.** (a) Curve fitting to the pseudo-first-order kinetic model, (b) the pseudo-second-order kinetic model, and (c) the Elovich model for the adsorption on activated carbon

As can be seen from Fig. 5 and Table 1, the pseudo-second-order kinetic model achieved the highest fitting correlation coefficient ($R^2 = 0.9987$). Further, the relative error between the fitted $Q_e$ (31.9 mg × $g^{-1}$) and the experimentally measured $Q_e$ (33.5 mg × $g^{-1}$) was small. The adsorption principle of trichlorophenol by activated carbon is mainly physical adsorption. Nut shell activated carbon has high specific surface area and unique pore structure; this is the most important reason for its adsorption of 2,4,6-TCP. The tiny pores in activated carbon have a strong adsorption capacity and can absorb substances with a diameter smaller than its pore size. The effect of adsorption time on removal rate of 2,4,6-TCP was studied. It can be found that 2,4,6-TCP adsorption can be divided into three stages: the diffusion of the outer liquid film, the adsorption rate increases rapidly; the adsorption rate decreased obviously in the particle diffusion stage; the adsorption equilibrium phase (Chang and Juang 2004). Thus, it reflected the adsorption mechanism of 2,4,6-TCP on activated carbon more comprehensively and accurately.

## Adsorption Isotherms

The adsorption of 2,4,6-TCP on activated carbon was analyzed using Langmuir, Freundlich, and Temkin isotherms (Muhamad *et al.* 2010; Moussa *et al.* 2018). The fitting equations and linear correlation coefficients are listed in Table 2. The equations of the Langmuir isotherm (Eq. 6), the Freundlich isotherm (Eq. 7), and the Temkin isotherm (Eq. 8) are as follows,

$$C_e / Q_e = 1 / (Q_m \times k_L) + C_e / Q_m \quad R_L = 1 / (1 + k_L \times C_0) \tag{6}$$

$$\ln Q_e = \ln k_F + (1 / n)\ln C_e \tag{7}$$

$$Q_e = B\ln k_T + B\ln C_e \quad B = RT / Z \tag{8}$$

where $k_L$ (L × mg$^{-1}$) is the reciprocal of the equilibrium concentration at half-saturated adsorption capacity. $Q_m$ (mg × g$^{-1}$) is the saturation adsorption capacity. $C_e$ (mg × L$^{-1}$) is the adsorption equilibrium concentration. $Q_e$ (mg × g$^{-1}$) is the equilibrium concentration of the solid phase. $R_L$ is used to estimate the pros and cons of adsorption. $C_0$ (mg × L$^{-1}$) is the initial concentration of adsorbate. $k_F$ and $n$ are the Freundlich constants. $B$ and $k_T$ are the Temkin adsorption constants. $R$ is the gas constant (R = 8.314 J × mol$^{-1}$ × K$^{-1}$). $T$ (K) is the absolute temperature. $Z$ (J.mol$^{-1}$) is the heat of adsorption.

Table 2 shows that the R$^2$ values of the fittings to the Langmuir and Freundlich adsorption isotherms at each temperature were greater than 0.98. These results indicated that the adsorption of 2,4,6-TCP on activated carbon was more consistent with the Langmuir and Freundlich adsorption isotherm models. This was likely because the Temkin model is suitable for adsorption with a medium coverage but not with a large coverage. The Freundlich model considers that the adsorbent surface is uneven, and the adsorption heat decreases exponentially with increasing coverage. Indeed, the surface of the adsorbent (activated carbon) was not uniform, and there existed a certain force between the 2,4,6-TCP molecules. Therefore, the Freundlich model gave a better fit of the data. Moreover, the value of 1/n in the Freundlich model was less than 0.5 at all temperatures, which suggested that the activated carbon was a good adsorbent for 2,4,6-TCP. The value of $R_L$ in the Langmuir adsorption model was between 0 and 1, which indicated that the adsorption of 2,4,6-TCP on activated carbon was relatively easy. However, the Langmuir adsorption model assumes that the adsorbent surface is uniform, and the adsorption energy is equal for the entire surface. Moreover, interaction between the adsorbent molecules is ignored (Yazdanbakhsh *et al.* 2018). Thus, the curve fitting to the Langmuir model was poorer than the curve fitting to the Freundlich model. In conclusion, the adsorption of 2,4,6-TCP on activated carbon showed better fits to the Langmuir and Freundlich models. The higher correlation coefficients for various temperatures obtained with the Freundlich model suggested that this model simulated the isothermal adsorption more accurately.

**Table 2.** Isotherm Parameters for 2,4,6-TCP Adsorption on Activated Carbon at Different temperatures

| Model | Parameter | 25 °C | 35 °C | 50 °C |
|---|---|---|---|---|
| Langmuir | Equation<br>R$^2$ | $\frac{Ce}{Qe}=\frac{Ce}{56.98}+\frac{1}{81.20}$<br>0.9799 | $\frac{Ce}{Qe}=\frac{Ce}{55.13}+\frac{1}{96.37}$<br>0.9866 | $\frac{Ce}{Qe}=\frac{Ce}{53.65}+\frac{1}{100.80}$<br>0.9802 |
| | $Q_m$ (mg × g$^{-1}$) | 56.98 | 55.13 | 53.65 |
| | $k_L$ | 1.425 | 1.748 | 1.879 |
| | $R_L$ | 0.066 | 0.054 | 0.051 |
| Freundlich | Equation<br>R$^2$ | $\ln Q_e = 0.4564\ln C_e + 3.135$<br>0.9966 | $\ln Q_e = 0.4464\ln C_e + 3.155$<br>0.9832 | $\ln Q_e = 0.4435\ln C_e + 3.163$<br>0.9879 |
| | $k_F$ | 22.98 | 23.45 | 23.64 |
| | 1/$n$ | 0.4564 | 0.4464 | 0.4435 |
| Temkin | Equation<br>R$^2$ | $Q_e = 7.680\ln C_e + 33.05$<br>0.9275 | $Q_e = 7.432\ln C_e + 33.29$<br>0.9417 | $Q_e = 7.369\ln C_e + 32.91$<br>0.9509 |
| | $k_T$ | 73.81 | 88.18 | 87.07 |
| | $B$ | 7.680 | 7.432 | 7.369 |

## Adsorption Thermodynamics

The thermodynamics of adsorption of 2,4,6-TCP on activated carbon were studied. The thermodynamic parameters were calculated using the Gibbs equation (Tran *et al.* 2016). The following other equations (Eq. 9, Eq. 10, Eq. 11, and Eq. 12) were used,

$$\Delta G^0 = -RT\ln K_d \tag{9}$$

$$K_d = Q / C \tag{10}$$

$$\ln K_d = \Delta S^0 / R - \Delta H^0 / RT \tag{11}$$

$$\Delta G^0 = \Delta H^0 - T\Delta S^0 \tag{12}$$

where $R$ (8.314 J × mol$^{-1}$ × K$^{-1}$) is the gas constant. $K_d$ is the thermodynamic equilibrium constant (adsorption coefficient). $T$ (K) is the absolute temperature.

**Table 3.** Thermodynamic Parameters for 2,4,6-TCP Adsorption on Activated Carbon

| $\Delta H^0$ (kJ × mol$^{-1}$) | $\Delta S^0$ (J × mol$^{-1}$ × K$^{-1}$) | $\Delta G^0$ (kJ × mol$^{-1}$) | | |
|---|---|---|---|---|
| | | 298 K | 308 K | 323 K |
| -26.27 | -48.18 | -11.91 | -11.43 | -10.71 |

The experimental results predicted a linear relationship between $\ln K_d$ and $1/T$ ($\ln K_d = 3.16 / T - 5.80$). The values of $\Delta H^0$ and $\Delta S^0$ were calculated to be -26.3 kJ × mol$^{-1}$ and -48.2 J × mol$^{-1}$ × K$^{-1}$, respectively. The value of $\Delta G^0$ was calculated at different temperatures. The details are given in Table 3. The adsorption enthalpy ($\Delta H^0$) was negative, which indicated that the adsorption of 2,4,6-TCP on activated carbon was an exothermic process. In addition, the adsorption was mainly divided into two processes, which were the desorption of solvent water molecules on the surface of activated carbon and the adsorption of 2,4,6-TCP. The former process increases the randomness of the reaction system, which results in a positive entropy. The latter is the reverse process, which decreases randomness and results in negative entropy. The value of $\Delta S^0$ was negative for the present system, which suggested that the adsorption was mainly governed by the adsorption of 2,4,6-TCP. The adsorption of 2,4,6-TCP on activated carbon reduced the randomness of the whole reaction system (Prajapati *et al.* 2016). In addition, $\Delta G^0$ was negative at different temperatures, which indicated that the adsorption of 2,4,6-TCP was spontaneous. An increase in the temperature led to a continuous decrease in the absolute value of $\Delta G^0$, which showed that adsorption was not favorable at high temperatures. Thus, the adsorption of 2,4,6-TCP on activated carbon was a spontaneous exothermic process.

## CONCLUSIONS

1. The effects of activated carbon dosage, adsorption time, and temperature on the adsorption of 2,4,6-TCP were studied, and the optimum adsorption conditions were obtained. The removal of 2,4,6-TCP was 91.5% under the optimal conditions.
2. The adsorption mechanism involved many different processes. A higher correlation coefficient was obtained at various temperatures with the Freundlich model, which suggested that this model simulated the adsorption more accurately. The adsorption of 2,4,6-TCP is a spontaneous exothermic process. This study provided a theoretical basis for AOX removal in natural environments.

## ACKNOWLEDGMENTS

The project was supported by the State Key Laboratory of Biobased Material and Green Papermaking (No. KF201808), Qilu University of Technology, and the Shandong Academy of Sciences. In addition, this project was sponsored by the National Natural Science Foundation of China (21968004 & 31760192).

## REFERENCES CITED

Amstaetter, K., Eek, E., and Cornelissen, G. (2012). “Sorption of PAHs and PCBs to activated carbon: Coal *versus* biomass-based quality,” *Chemosphere* 87(5), 573-578. DOI: 10.1016/j.chemosphere.2012.01.007

Bhatnagar, A., Hogland, W., Marques, M., and Sillanpää, M. (2013). “An overview of the modification methods of activated carbon for its water treatment applications,” *Chemical Engineering Journal* 219, 499-511. DOI: 10.1016/j.cej.2012.12.038

Ceyhan, A. A., Şahin, Ö., Saka, C., and Yalçın, A. (2013). “A novel thermal process for activated carbon production from the vetch biomass with air at low temperature by two-stage procedure,” *Journal of Analytical and Applied Pyrolysis* 104, 170-175. DOI: 10.1016/j.jaap.2013.08.007

Chang, M.-Y., and Juang, R.-S. (2004). “Adsorption of tannic acid, humic acid, and dyes from water using the composite of chitosan and activated clay,” *Journal of Colloid and Interface Science* 278(1), 18-25. DOI: 10.1016/j.jcis.2004.05.029

Deshmukh, N. S., Lapsiya, K. L., Savant, D. V., Chiplonkar, S. A., Yeole, T. Y., Dhakephalkar, P. K., and Ranade, D. R. (2009). “Upflow anaerobic filter for the degradation of adsorbable organic halides (AOX) from bleach composite wastewater of pulp and paper industry,” *Chemosphere* 75(9), 1179-1185. DOI: 10.1016/j.chemosphere.2009.02.042

Fernandez, M. E., Nunell, G. V., Bonelli, P. R., and Cukierman, A. L. (2014). “Activated carbon developed from orange peels: Batch and dynamic competitive adsorption of basic dyes,” *Industrial Crops and Products* 62, 437-445. DOI: 10.1016/j.indcrop.2014.09.015

Francis, D. W., Turner, P. A., and Wearing, J. T. (1997). “AOX reduction of kraft bleach plant effluent by chemical pretreatment—Pilot-scale trials,” *Water Research* 31(10), 2397-2404. DOI: 10.1016/S0043-1354(97)00058-4

Ge, J., Wu, Y., Han, Y., Qin, C., Nie, S., Liu, S., Wang, S., and Yao, S. (2020). “Effect of hydrothermal pretreatment on the demineralization and thermal degradation behavior of eucalyptus,” *Bioresource Technology* 307, 123246. DOI: 10.1016/j.biortech.2020.123246

Hameed, B. H., Tan, I. A. W., and Ahmad, A. L. (2008). “Adsorption isotherm, kinetic modeling and mechanism of 2,4,6-trichlorophenol on coconut husk-based activated carbon,” *Chemical Engineering Journal* 144(2), 235-244. DOI: 10.1016/j.cej.2008.01.028

Huang, L., Yang, Z., Li, M., Liu, Z., Qin, C., Nie, S., and Yao, S. (2020). “Effect of pre-corrected pH on the carbohydrate hydrolysis of bamboo during hydrothermal pretreatment,” *Polymers* 12(3), 612-628. DOI: 10.3390/polym12030612

Jaacks, L. M., and Staimez, L. R. (2015). “Association of persistent organic pollutants and non-persistent pesticides with diabetes and diabetes-related health outcomes in

Asia: A systematic review," *Environment International* 76, 57-70. DOI: 10.1016/j.envint.2014.12.001

Kadirvelu, K., Thamaraiselvi, K., and Namasivayam, C. (2001). "Removal of heavy metals from industrial wastewaters by adsorption onto activated carbon prepared from an agricultural solid waste," *Bioresource Technology* 76(1), 63-65. DOI: 10.1016/S0960-8524(00)00072-9

Kavitha, D., and Namasivayam, C. (2007). "Experimental and kinetic studies on methylene blue adsorption by coir pith carbon," *Bioresource Technology* 98(1), 14-21. DOI: 10.1016/j.biortech.2005.12.008

Krawczyk, H., Oinonen, P., and Jönsson, A. S. (2013). "Combined membrane filtration and enzymatic treatment for recovery of high molecular mass hemicelluloses from chemithermomechanical pulp process water," *Chemical Engineering Journal* 225, 292-299. DOI: 10.1016/j.cej.2013.03.089

Liu, B., Qin, C., Zhang, F., Wang, S., Liang, C., Nie, S., Wang, S., and Yao, S. (2020). "Reaction mechanism of phenolic lignin and high concentration chlorine dioxide and its application," *ACS Omega* 5, 22475-22481. DOI: 10.1021/acsomega.0c03028

Moussa, M., Bader, N., Querejeta, N., Duràn, I., Pevida, C., and Ouederni, A. (2018). "$CO_2$ adsorption on activated carbon based olive stone: A comparison of Langmuir and Freundlich models," in: *Recent Advances in Environmental Science from the Euro-Mediterranean and Surrounding Regions*, A. Kallel, M. Ksibi, H. Ben Dhia, N. Khélifi (eds.), Springer International Publishing, Cham, Switzerland, pp. 1099-1100.

Muhamad, H., Doan, H. D., and Lohi, A. (2010). "Batch and continuous fixed-bed column biosorption of $Cd^{2+}$ and $Cu^{2+}$," *Chemical Engineering Journal* 158(3), 369-377. DOI: 10.1016/j.cej.2009.12.042

Nie, S., Liu, X., Wu, Z., Zhan, L., Yin, G., Yao, S., Song, H., and Wang, S. (2014). "Kinetics study of oxidation of the lignin model compounds by chlorine dioxide," *Chemical Engineering Journal* 241, 410-417. DOI: 10.1016/j.cej.2013.10.068

Nie, S., Zhang, K., Lin, X., Zhang, C., Yan, D., Liang, H., and Wang, S. (2018). "Enzymatic pretreatment for the improvement of dispersion and film properties of cellulose nanofibrils," *Carbohydrate Polymers* 181, 1136-1142. DOI: 10.1016/j.carbpol.2017.11.020

Prajapati, Y. N., Bhaduri, B., Joshi, H. C., Srivastava, A., and Verma, N. (2016). "Aqueous phase adsorption of different sized molecules on activated carbon fibers: Effect of textural properties," *Chemosphere* 155, 62-69. DOI: 10.1016/j.chemosphere.2016.04.040

Shi, L., Ge, J., Nie, S., Qin, C., and Yao, S. (2019). "Effect of lignin structure on adsorbable organic halogens formation in chlorine dioxide bleaching," *Royal Society Open Science* 6, 182024. DOI: 10.1098/rsos.182024

Savant, D. V., Abdul-Rahman, R., and Ranade, D. R. (2006). "Anaerobic degradation of adsorbable organic halides (AOX) from pulp and paper industry wastewater," *Bioresource Technology* 97(9), 1092-1104. DOI: 10.1016/j.biortech.2004.12.013

Shih, T. C., Wangpaichitr, M., and Suffet, M. (2003). "Evaluation of granular activated carbon technology for the removal of methyl tertiary butyl ether (MTBE) from drinking water," *Water Research* 37(2), 375-385. DOI: 10.1016/s0043-1354(02)00271-3

Šmídová, K., Kim, S., and Hofman, J. (2017). "Bioavailability of five hydrophobic organic compounds to earthworms from sterile and non-sterile artificial soils," *Chemosphere* 179, 222-231. DOI: 10.1016/j.chemosphere.2017.03.117

Terrell, E., Dellon, L. D., Dufour, A., Bartolomei, E., Broadbelt, L. J., and Garcia-Perez, M. (2020). "A review on lignin liquefaction: Advanced characterization of structure and microkinetic modeling," *Industrial and Engineering Chemistry Research* 59(2), 526-555. DOI: 10.1021/acs.iecr.9b05744

Tran, H. N., You, S.-J., and Chao, H.-P. (2016). "Thermodynamic parameters of cadmium adsorption onto orange peel calculated from various methods: A comparison study," *Journal of Environmental Chemical Engineering* 4(3), 2671-2682. DOI: 10.1016/j.jece.2016.05.009

Tan, I. A. W., Ahmad, A. L., and Hameed, B. H. (2009). "Adsorption isotherms, kinetics, thermodynamics and desorption studies of 2,4,6-trichlorophenol on oil palm empty fruit bunch-based activated carbon," *Journal of Hazardous Materials* 164(2-3), 473-482. DOI: 10.1016/j.jhazmat.2008.08.025

Vikrant, K., Kim, K.-H., Kumar, S., and Boukhvalov, D. W. (2020). "Metal–organic frameworks for the adsorptive removal of gaseous aliphatic ketones," *ACS Applied Materials and Interfaces* 12(9), 10317-10331. DOI: 10.1021/acsami.9b20375

Wirasnita, R., Mori, K., and Toyama, T. (2018). "Effect of activated carbon on removal of four phenolic endocrine-disrupting compounds, bisphenol A, bisphenol F, bisphenol S, and 4-tert-butylphenol in constructed wetlands," *Chemosphere* 210, 717-725. DOI: 10.1016/j.chemosphere.2018.07.060

Yazdanbakhsh, A., Eslami, A., Moussavi, G., Rafiee, M., and Sheikhmohammadi, A. (2018). "Photo-assisted degradation of 2,4,6-trichlorophenol by an advanced reduction process based on sulfite anion radical: Degradation, dechlorination and mineralization," *Chemosphere* 191, 156-165. DOI: 10.1016/j.chemosphere.2017.10.023

You, F.-T., Yu, G.-W., Wang, Y., Xing, Z.-J., Liu, X.-J., and Li, J. (2017). "Study of nitric oxide catalytic oxidation on manganese oxides-loaded activated carbon at low temperature," *Applied Surface Science* 413, 387-397. DOI: 10.1016/j.apsusc.2017.04.044

Yao, S., Nie, S., Yuan, Y., Wang, S., and Qin, C. (2015). "Efficient extraction of bagasse hemicelluloses and characterization of solid remainder," *Bioresource Technology* 185, 21-27. DOI: 10.1016/j.biortech.2015.02.052

Yao, S., Gao, C., Zhu, H., Zhang, Y., Wang, S., and Qin, C. (2016). "Effects of additives on absorbable organic halide reduction in elemental chlorine-free bleaching of bagasse kraft pulp," *BioResources* 11(1), 996-1006. DOI: 10.15376/biores.11.1.996-1006

Yao, S., Nie, S., Zhu, H., Wang, S., Song, X., and Qin, C. (2017). "Extraction of hemicellulose by hot water to reduce adsorbable organic halogen formation in chlorine dioxide bleaching of bagasse pulp," *Industrial Crops and Products* 96, 178-185. DOI: 10.1016/j.indcrop.2016.11.046

Zhang, G., He, Z., and Xu, W. (2012). "A low-cost and high efficient zirconium-modified-Na-attapulgite adsorbent for fluoride removal from aqueous solutions," *Chemical Engineering Journal* 183, 315-324. DOI: 10.1016/j.cej.2011.12.085

Zhang, H., Nie, S., Qin, C., and Wang, S. (2019). "Removal of hexenuronic acid to reduce AOX formation in hot chlorine dioxide bleaching of bagasse pulp," *Industrial Crops and Products* 128, 338-345. DOI: 10.1016/j.indcrop.2018.11.025

Zhang, Z., Shan, Y., Wang, J., Ling, H., Zang, S., Gao, W., Zhao, Z., and Zhang, H. (2007). "Investigation on the rapid degradation of congo red catalyzed by activated carbon powder under microwave irradiation," *Journal of Hazardous Materials* 147(1-2), 325-333. DOI: 10.1016/j.jhazmat.2006.12.083

Article submitted: June 16, 2020; Peer review completed: August 23, 2020; Revised version received and accepted: August 24, 2020; Published: October 9, 2020.
DOI: 10.15376/biores.15.4.8800-8812